An Unified Virtual Battery Modeling Framework for Flexibility Characterization of Building HVAC Systems

Qi Zhu, Yu Yang, *Member, IEEE,* Liang Yu, *Senior Member, IEEE,* Qing-Shan Jia, *Senior Member, IEEE,*
Costas J. Spanos, *Fellow, IEEE,* Xiaohong Guan, *Life Fellow, IEEE*

Abstract—The heating, ventilation and air-conditioning (HVAC) system dominates building's energy consumption and meanwhile exhibits substantial operational flexibility that can be exploited for providing grid services. However, the goal is largely hindered by the difficulty to characterize the system's operating flexibility due to the complex building thermal dynamics, system operating limits and human comfort constraints. To address this challenge, this paper develops an unified virtual battery (VB) modeling framework for characterizing the operating flexibility of both single-zone and multi-zone building HVAC systems, enabling flexible buildings to function like virtual batteries. Specifically, a physically meaningful representation state is first identified to represent building thermal conditions under thermal comfort constraints and a VB model is then established for characterizing the operating flexibility of single-zone HVAC systems. We subsequently extend the VB modeling framework to multi-zone HVAC systems and establish a set of zone-level VB models to characterize the building's zonal operating flexibility. We further develop a systematic method to aggregate the VB models into a low-order and low-complexity aggregated VB model, significantly reducing model and computational complexity. We demonstrate the VB model through demand response (DR) applications and conclude that the VB model can well capture the operating flexibility of building HVAC systems and enable effective DR participation. The DR strategies obtained from the VB model can be efficiently decomposed to zone-level control inputs for maintaining human thermal comfort while achieving near-optimal operation cost.

Index Terms—multi-zone HVAC systems, virtual battery (VB) model, flexibility characterization, building-level energy management and scheduling, low-complexity.

I. INTRODUCTION

BUILDINGS account for over 35% of global energy consumption, while the heating, ventilation, and air conditioning (HVAC) systems for space conditioning contribute about 40%–50% of buildings' total energy use [1]. Particularly,

Q. Zhu and Y. Yang are with School of Automation Science and Engineering, Xi'an Jiaotong University, Shaanxi, Xi'an 710049, China (e-mail: zhuqi@stu.xjtu.edu.cn, yangyu21@xjtu.edu.cn). *Y. Yang is the corresponding author.*

L. Yu is with the College of Automation, Nanjing University of Posts and Telecommunications, Nanjing 210023, China (e-mail: liang.yu@njupt.edu.cn).

Q. -S. Jia is with the Center for Intelligent and Networked Systems, Department of Automation, BNRist, Tsinghua University, Beijing 100084, China (e-mail: jiaqs@tsinghua.edu.cn).

X. Guan is with School of Automation Science and Engineering, Xi'an Jiaotong University, Shaanxi, Xi'an 710049, China, and also with the Center for Intelligent and Networked Systems, Department of Automation, Tsinghua University, Beijing 100084, China (e-mail: xhguan@tsinghua.edu.cn).

C. J. Spanos is with the Department of Electrical Engineering and Computer Sciences, University of California, Berkeley, CA, 94720 USA (email: spanos@berkeley.edu).

this proportion is continuing increasing and projected to grow by more than 50% by 2050 [2]. As the main energy sector, buildings' energy consumption shows substantial operating flexibility due to the buildings' thermal inertia and wide comfortable temperature ranges of occupants. Specifically, the thermal energy generated by HVAC units can be temporally and bidirectionally modulated in response to power grid operating requirements. Building HVAC systems have been recognized as one of the most important flexible resources for alleviating the flexibility shortage of modern power grids [3] and providing a wide range of grid services, including demand response [4], peak shaving [5], frequency regulation [6], etc.

The exploitation of operating flexibility of building HVAC systems rely on tractable models for flexibility characterization. Considerable efforts have been made for developing models for capturing building thermal dynamics under HVAC control inputs. The existing models can be broadly classified into white-box, black-box and gray-box models (see [7] for a comprehensive review). White-box models depend on professional simulators, such as EnergyPlus [8] and TRNSYS [9], to capture the detailed physical principles and emulate real operating scenarios. Back-box models generally employ common expressive functional modules, such as neural networks [10], linear regression models [11], to capture the complex mappings between HVAC control inputs, external thermal disturbances and building thermal dynamics. The models often involve a large number of parameters and require high-quality operating data for model parameter identification. In contrast, gray-box models generally rely on simplified physical principles, such as energy and mass conservation, heat transfer and convection principles, for mathematical models establishment, enjoying the benefit of limited model parameters and high model generality. Among the existing models, the resistor–capacitor (RC) models that employ thermal resistance and capacitance to characterize heat transfer efficiency and the thermal inertia of building components [12, 13], have been most widely used for control-oriented applications (see [14, 15] for examples) due to their high interpretability.

However, most of the existing models for thermal dynamics modeling for building HVAC system are not suitable for characterizing the system's operating flexibility. They are often subject to high-dimensional nonlinear thermal dynamics, operating limits and human comfort constraints. When considering the unlock of building operating flexibility for mangy high-level energy management or scheduling tasks, a low-order and low-complexity model that provides the energy scheduling boundaries would be preferred rather than a detailed zone-level control models that are computationally intensive.
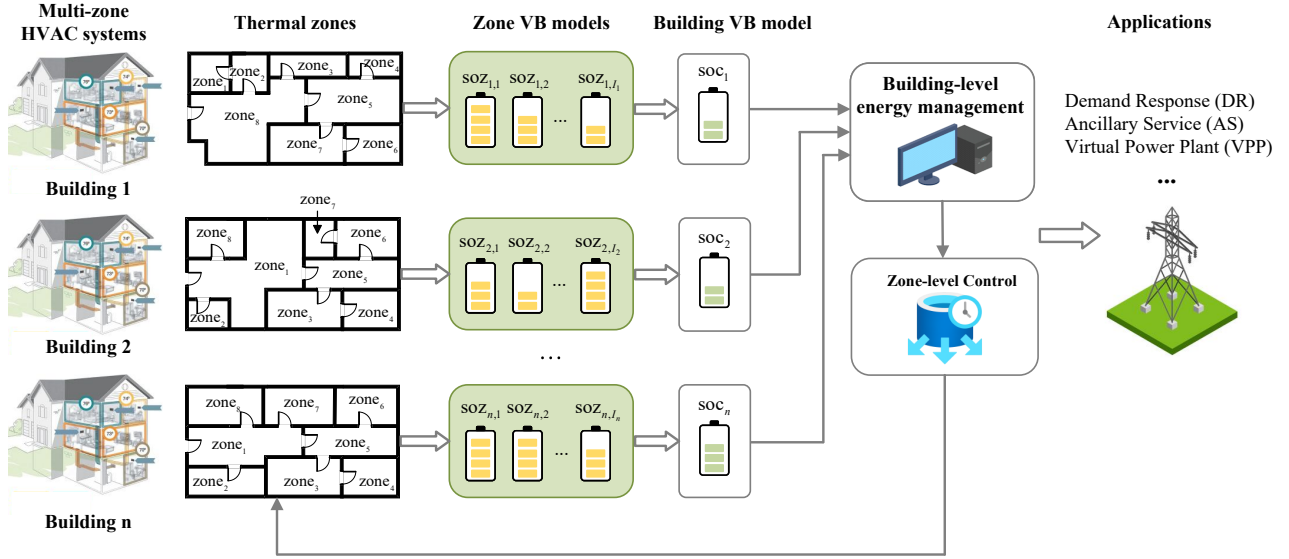
Fig. 1: VB model for characterizing operating flexibility of building HVAC systems

To this end, many researches has focused on developing low-order and low-complexity models for characterizing the operating flexibility of building HVAC systems. For single-zone HVAC systems (often used in residential buildings), numerous studies have developed virtual battery (VB) models for characterizing their operating flexibility that show high interpretability and are easy to be coordinated. Whereas the problem is much more complicated and challenging with multi-zone HVAC systems (often used in commercial buildings) that show quite different operating behaviors and admit high-dimensional nonlinear state-space formulations. To address this challenge, several studies have relied on data-driven approaches to capture the aggregated operating flexibility of multi-zone HVAC systems [16, 17]. Whereas the model constructions are very sophisticated and lack of theoretical guarantee. A number of works have developed optimization-based methods to approximate the system's operating flexibility by virtual battery representation, but depend on solving a sequence of comprehensive optimization problems for model parameter identification [18]. From the literature, we find that characterizing the operating flexibility for building HVAC systems is a nontrivial problem and a systematic approach is still lacking.

To fill the gap, this paper develops a virtual battery framework to characterize the operational flexibility for both single-zone and multi-zone building HVAC systems. The VB models are established from the well-known RC formulations via equivalent mathematical transformations, thus with readily available model parameters and theoretic guarantee. Particularly, the VB models provide high interpretability and enable flexible buildings to function like virtual batteries when interact with the power grid operators. A schematic illustration of our idea is presented in Fig. 1. The VB models are applicable to a wide range of building-level and cluster-level energy management and scheduling tasks while leveraging buildings' operating flexibility. **The main contributions of this paper are summarized as follows**:

- We propose a compact and physically meaningful *characterization state* to represent building thermal conditions under thermal comfort constraints, and further establish a VB model for characterizing the operational flexibility of single-zone building HVAC systems.
- We extend the VB modeling framework to multi-zone building HVAC systems and establish a set of zone-level VB models to capture the heterogeneous zonal thermal dynamics and operating flexibility.
- We further develop a systematic method for aggregating the zone-level VB models into a low-order and low-complexity aggregated VB model, significantly reducing model and computational complexity.

We demonstrate the effectiveness of VB models through demand response (DR) applications. The results show that the low-order and low-complexity VB models can well capture the thermal dynamics of buildings under varying HVAC control and can enable effective DR participation. The rest of this paper is summarized: In Section II, we review the related works on the operating flexibility characterization and modeling of building HVAC systems; In section III and IV, we introduce the VB models for single-zone and multi-zone HVAC systems. In Section V, the VB models are validated and tested for DR applications. In Section VI, we conclude this paper and discuss future works.

II. LITERATURE

A substantial body of researches has focused on the operating flexibility characterization of building HVAC systems. Existing works as well as this paper are contrasted in Table I, including the types of systems considered (`Systems`), the approaches used to build the models (`Methods`), the resulted model formulations (`Models`), the computational complexity of the model parameters identification (`Model Complexity`), and theoretical guarantee of model accuracy (`Theoretic Guarantee`).

TABLE I: Existing works of flexibility characterization for building HVAC systems

Systems	Methods	Models	Method complexity	Theoretic Guarantee	Year	Paper
Multi-zone HVAC Single-zone HVAC	Optimization-based	Generalized Battery Model	High	No	2017	[18]
Single-zone HVAC	Optimization-based	Polytope	High	No	2017, 2025	[19, 20]
Single-zone HVAC	Data-driven	Linear regression	Low	No	2021, 2024	[11, 21]
Single-zone HVAC	Model-based	Virtual Battery Model	Low	Yes	2017, 2019	[22, 23]
Single-zone HVAC	Model-based	Virtual Battery Model	Low	Yes	2025	[24]
Multi-zone HVAC	Data-driven	Virtual Storage Model	High	No	2024	[16]
Multi-zone HVAC	Data-driven	Neural Network	High	No	2024	[17]
Multi-zone HVAC	Model-based	Virtual Battery Model	Low	No	2022	[25]
Multi-zone HVAC	Model-based	2R2C	Low	No	2019,2021	[26, 27]
Multi-zone HVAC Single-zone HVAC	**Model-based**	**Virtual Battery Model**	**Low**	**Yes**	**2025**	**This paper**

The existing works mainly focused on single-zone and multi-zone HVAC, respectively. This is mainly because the two types of systems operate quite differently and show different operating behaviors. The former typically operates with constant ventilation rates and admits linear state-space models, while the later generally operates with variable ventilation rates and depend on high-dimensional and non-linear state-space model for capturing spatially-temporally coupled thermal dynamics. The approaches can be classified into optimization-based, data-driven and model-based. Optimization-based methods are generally about identifying a group of parameters for user-defined characterization models, including virtual battery models [18] or polytope models [19, 20], to approximate the operating flexibility of building HVAC systems. These approaches are usually computationally intensive as a sequence of comprehensive optimization problems are required to be solved for model parameters identification. Data-driven approaches generally share the idea of using functional modules to approximate the buildings' thermal dynamics, including piece-wise linear (PWL) functions [16], linear regression models [11, 21] and neural networks [17], etc. Data-driven approaches are advantageous in handling the complex system dynamics but the resulted models often lack generality and theoretic guarantee. In contrast, model-based methods generally proposed to establish characterization models from existing building thermal dynamic models, typically the RC formulations, via analytic or mathematical transformations (see [22, 23] for examples). They often provide interpretability and theoretic soundness.

This above methods have led to a set of characterization models, including virtual energy storage (VES) or virtual battery (VB) models, polytopes, linear regression models and neural networks, among others. The VES and VB models have been widely employed mainly due to their natural capability for flexibility characterization and easy to be co-ordinated with other types of energy storage systems. For single-zone HVAC, a number of studies has developed VB models for characterizing the system's operating flexibility [22–24]. Whereas the issue with multi-zone HVAC systems

has been largely unresolved. This is mainly due to the systems' complicated and quite different operating behaviors, leading to high-dimensional and nonlinear state-space models. This makes the development of low-order models for capturing and aggregating the zonal flexibility mathematically complicated. Notably, [18, 25] proposed to characterize the flexibility of multi-zone HVAC by VES models using optimization-based techniques to identify model parameters. [16] proposed to train PWL functions to approximate the non-linear and complicated thermal dynamics for VES modeling. Slightly different, [17] proposed to learn a low-order model in the latent space using machine learning techniques to overcome the model complexity. [26, 27] have derived an aggregated RC model from the original RC formulations for multi-zone HVAC systems, but face the difficulty to handle model parameters as they are closely coupled with zone-level state and decision variables.

From the literature, we find that many efforts have been made for flexibility characterization of building HVAC systems, driven by the growing demand to unlock the enormous flexibility for supporting modern power operation. However, the problem is still largely unresolved and there still lacks a systematic framework account for both single-zone and multi-zone HVAC systems. Moreover, existing works mostly relied on optimization-based and data-driven approaches for model constructions, suffering from high computational complexity in model parameters identification, limited generality and theoretic guarantee.

III. VIRTUAL BATTERY MODEL FOR SINGLE-ZONE HVAC

For single-zone HVAC systems that are typically used in residential buildings, the widely used resistor-capacitor (RC) models take the formulation of [18, 28].

$$C_n^{\text{th}} \left(T_n(k+1) - T_n(k) \right) = \frac{T^{\text{out}}(k) - T_n(k)}{R_{n,o}^{\text{th}}} \Delta k$$
$$- \eta_n^{\text{HVAC}} q_n^{\text{HVAC}}(k) \Delta k + Q_n^{\text{dist}}(k) \Delta k, \quad (1a)$$

$$q_n^{\text{HVAC,min}} \leq q_n^{\text{HVAC}}(k) \leq q_n^{\text{HVAC,max}}, \quad (1b)$$

$$T_n^{\text{set}} - \delta_n \leq T_n(k) \leq T_n^{\text{set}} + \delta_n, \quad \forall k \in \mathcal{K}. \quad (1c)$$

where n and k are building and time index. Equations (1a) represent zone thermal dynamics. C_n^{th} is zone thermal capacity, $T_n(k)$ is zone air temperature, $T^{\text{out}}(k)$ is outdoor temperature, T_n^{sup} denotes the setpoint temperature of supplied airflow, $R_{n,o}^{\text{th}}$ represents the thermal resistance between the zone and the outside, $Q_{n,i}^{\text{dist}}(k)$ denotes the thermal disturbances caused by occupants, electrical devices and solar radiations, etc. $q_n^{\text{HVAC}}(k)$ denotes the controllable power consumption of the HVAC unit, with η_n^{HVAC} denoting the chiller's coefficient of performance (COP). Constraints (1b) specify the feasible range of HVAC power consumption, with $q_n^{\text{HVAC,min}}$ and $q_n^{\text{HVAC,max}}$ denoting the lower and upper limits. Constraints (1c) model human thermal comfort, with T_n^{set} denoting the ideal zone temperature setpoint and δ_n indicating the allowable upward and downward deviation. Note that the single-zone HVAC systems that typically operate in constant ventilation rates, admit linear state-space models. The zone thermal dynamics (1a) can be stated in a compact format:

$$T_n(k+1) = a_n T_n(k) - b_n q_n^{\text{HVAC}}(k) + d_n(k), \forall k \in \mathcal{K}. \quad (2)$$

where we have $a_n = 1 - \Delta k/(C_n^{\text{th}} R_{n,o}^{\text{th}})$, $b_n = \eta^{\text{HVAC}}/C_n^{\text{th}} \Delta k$ and $d_n(k) = T^{\text{out}}(k)\Delta k/(C_n^{\text{th}} R_{n,o}^{\text{th}}) + Q_n^{\text{dist}}(k)\Delta k/C_n^{\text{th}}$.

A. Characterization State

Before establishing the VB model, we first define the following state-of-zone (soz) as the *characterization state* of zone thermal conditions under thermal comfort constraints:

$$\text{soz}_n(k) = \frac{T_n^{\text{set}} - T_n(k)}{\delta_n}, \quad \forall k \in \mathcal{K}. \quad (3)$$

Particularly, the soz can be viewed as "State-of-Comfort" of the zone. When the zone is controlled within the comfortable temperature range, it follows that $\text{soz}_n(k) \in [-1,1], k \in \mathcal{K}$. Meanwhile, the soz can be viewed as "State-of-Charge" of the zone, with the upper and lower limits 1 and -1 denoting a full and an empty zone state. Particularly, when the zone reaches lower temperature limit, it can not consume any energy further (i.e., charging) and we have a full zone indicated by soz $= 1$. Oppositely, when the zone reaches upper temperature limit, the zone can not reduce any energy consumption (i.e., discharging) and we have an empty zone indicated by soz $= -1$. The soz can be interpreted as the zone thermal conditions and is also the basis to establish a VB model from the RC formulation.

B. VB Model for Single-zone HVAC

For the operation of HVAC system, an ideal setting is to maintain zone temperature at the setpoints. We refer to this control policy as `Baseline control`, corresponding to the following steady state equations by (1a):

$$T_n^{\text{base}}(k+1) = a_n T_n^{\text{base}}(k) - b_n q_n^{\text{HVAC,base}}(k) + d_n(k), \forall k \in \mathcal{K}. \quad (4)$$

By subtracting (1a) from (4) and dividing δ_n, we have

$$\frac{T_n^{\text{base}}(k+1) - T_n(k+1)}{\delta_n} = a_n \frac{T_n^{\text{base}}(k) - T_n(k)}{\delta_n} + b_n(q_n^{\text{HVAC}}(k) - q_n^{\text{HVAC,base}}(k)), \quad \forall k \in \mathcal{K}. \quad (5)$$

By introducing the characterization state (3), we have

$$\text{soz}_n(k+1) = a_n \text{soz}_n(k) + P_n^{\text{ch/dis}}(k) \quad (6)$$

where $P_n^{\text{ch/dis}}(k) \triangleq b_n/\delta_n \left(q_n^{\text{HVAC}}(k) - q_n^{\text{HVAC,base}}(k)\right)$ can be viewed as the net charging power of a VB model.

By further encoding the operating and thermal comfort constraints (1b)-(1c) with $P_n^{\text{ch/dis}}(k)$ and $\text{soz}_n(k)$, we can obtain the following VB models for single-zone building HVAC systems:

VB model for single-zone HVAC:

$$\begin{cases} \text{soz}_n(k+1) = a_n \text{soz}_n(k) + P_n^{\text{ch/dis}}(k), \\ -1 \leq \text{soz}_n(k) \leq 1, \\ P_n^{\text{ch/dis}}(k) \geq q_n^{\text{HVAC,min}} - q_n^{\text{HVAC,base}}(k), \\ P_n^{\text{ch/dis}}(k) \leq q_n^{\text{HVAC,max}} - q_n^{\text{HVAC,base}}(k), \forall k \in \mathcal{K}. \end{cases} \quad (7)$$

For a single-zone HVAC system, the related energy consumption at time step k is $q_n^{\text{HVAC}}(k)\Delta k$, which can be equivalently expressed by

$$Q_n^{\text{tol}}(k) = (P_n^{\text{ch/dis}}(k)\delta_n/b_n + q_n^{\text{HVAC,base}}(k))\Delta k, \forall k \in \mathcal{K}. \quad (8)$$

with VB model (7).

IV. VIRTUAL BATTERY MODELS FOR MULTI-ZONE HVAC

This section discusses extension of the VB modeling framework to multi-zone building HVAC systems. This problem is non-trivial as the systems show much more complicated operating behaviors than single-zone cases. We refer the readers to [15, 29] for more details.

A. RC models for multi-zone HVAC systems

For multi-zone HVAC systems typically deployed in commercial buildings, the general RC formulations are [15, 30]:

$$C_{n,i}^{\text{th}}(T_{n,i}(k+1) - T_{n,i}(k)) = \sum_{j \in \mathcal{I}_n(i)} \frac{T_{n,j}(k) - T_{n,i}(k)}{R_{n,ij}^{\text{th}}} \Delta k$$
$$+ \frac{T^{\text{out}}(k) - T_{n,i}(k)}{R_{n,oi}^{\text{th}}} \Delta k + c_p m_{n,i}(k)(T_n^{\text{sup}} - T_{n,i}(k))\Delta k$$
$$+ Q_{n,i}^{\text{dist}}(k)\Delta k, \qquad \forall i \in \mathcal{I}_n, k \in \mathcal{K}. \quad (9a)$$
$$m_{n,i}^{\text{min}} \leq m_{n,i}(k) \leq m_{n,i}^{\text{max}}, \qquad \forall i \in \mathcal{I}_n, k \in \mathcal{K}. \quad (9b)$$
$$T_{n,i}^{\text{set}} - \delta_{n,i} \leq T_{n,i}(k) \leq T_{n,i}^{\text{set}} + \delta_{n,i}, \quad \forall i \in \mathcal{I}_n, k \in \mathcal{K}. \quad (9c)$$

where n, i, k are building, zone and time index. We use $\mathcal{I}_n$ and I_n to denote the set and number of zones involved. Equations (9a) represent the spatially-temporally coupled zone thermal dynamics. $R_{n,ij}$ denotes the thermal resistance between the adjacent zone i and zone j. $\mathcal{I}_n(i)$ denotes the set of zones adjacent to zone i. c_p is the specific heat of air. $m_{n,i}(k)$ denotes the zone airflow rates to be controlled. The other notations follow the single-zone case. Constraints (9b) specify the feasible ranges of zone airflow rates, with $m_{n,i}^{\text{min}}$ and $m_{n,i}^{\text{max}}$ denoting the minimum and maximum values determined by the VAV boxes operating limits. Constraints (9c) model

zone thermal comfort constraints. Similarly, the zone thermal dynamics (10) can be presented in a compact format:

$$T_{n,i}(k+1)=a_{n,ii}T_{n,i}(k)+\sum_{j\in\mathcal{I}_n(i)}a_{n,ij}T_{n,j}(k)+a_{n,i}^{\text{out}}T^{\text{out}}(k)$$
$$- b_{n,i}q_{n,i}(k) + d_{n,i}(k), \tag{10}$$
$$q_{n,i}(k) = c_p m_{n,i}(k)(T_{n,i}(k)-T_n^{\text{sup}}), \forall i \in \mathcal{I}_n, \forall k \in \mathcal{K}.$$

where the parameters $a_{n,ii}, a_{n,ij}, a_{n,i}^{\text{out}}, b_{n,i}, d_{n,i}(k)$ are

$$\begin{cases} a_{n,ii}=1-\Delta k/(R_{n,io}^{\text{th}}C_{n,i}^{\text{th}})-\sum_{j\in\mathcal{I}_n(i)}\Delta k/(R_{n,ij}^{\text{th}}C_{n,i}^{\text{th}}), & \forall i\in\mathcal{I}_n. \\ a_{n,ij} = \Delta k/(C_{n,i}^{\text{th}}R_{n,ij}^{\text{th}}), & \forall i,j\in\mathcal{I}_n. \\ a_{n,i}^{\text{out}} = \Delta k/(R_{n,io}^{\text{th}}C_{n,i}^{\text{th}}), & \forall i\in\mathcal{I}_n. \\ b_{n,i} = \Delta k/C_{n,i}^{\text{th}}, & \forall i\in\mathcal{I}_n. \\ d_{n,i}(k) = Q_{n,i}^{\text{dist}}(k)\Delta k/C_{n,i}^{\text{th}}, & \forall i\in\mathcal{I}_n, \quad k\in\mathcal{K}. \end{cases}$$

By stacking (10) across the thermal zones, we have the zone thermal dynamics of matrix format:

$$\boldsymbol{T}_n(k+1)=\boldsymbol{A}_n\boldsymbol{T}_n(k)-\boldsymbol{B}_n\boldsymbol{q}_n(k)+\boldsymbol{a}_n^{\text{out}}\boldsymbol{T}^{\text{out}}(k)+\boldsymbol{d}_n(k),$$
$$\boldsymbol{q}_n(k) = c_p \boldsymbol{m}_n(k)\left(\boldsymbol{T}_n(k) - \mathbf{1}_n T_n^{\text{sup}}\right), \forall k \in \mathcal{K}. \tag{11}$$

where we have

$$\boldsymbol{A}_n = \left[a_{n,ij}\right]_{i,j\in\mathcal{I}_n} \in R^{I_n\times I_n},$$
$$\boldsymbol{B}_n = \text{diag}(b_{n,1}, b_{n,2}, \ldots, b_{n,I_n}) \in R^{I_n\times I_n},$$
$$\mathbf{1}_n = [1, 1, \cdots, 1]^\mathsf{T} \in R^{I_n}.$$

The energy consumption of multi-zone HVAC systems consists of cooling power and fan power, which are [15, 30]

$$P_{\text{cooling}}(k) = c_p(1 - d_r) \sum_{i\in\mathcal{I}_n} m_{n,i}(k)(T^{\text{out}}(k) - T_n^{\text{sup}})$$
$$+ c_p d_r \sum_{i\in\mathcal{I}_n} m_{n,i}(k)(T_{n,i}(k) - T_n^{\text{sup}}), \tag{12}$$
$$P_{\text{fan}}(k) = \kappa_f \left(\sum_{i\in\mathcal{I}_n} m_{n,i}(k)\right)^2, \forall k \in \mathcal{K}.$$

where $d_r \in [0, 1]$ denotes the fraction of return air to AHU. The cooling power is divided into two parts: cooling the outdoor fresh air and the return air entering the AHU to the setpoint. The fan power is calculated by total zone airflow rates. The cooling power is generated by the chilled water pumped from the chiller and thus its electrical consumption is determined by affected the chiller's COP. Collectively, the system's total energy consumption can be expressed as

$$Q_n^{\text{tol}}(k) = P_{\text{cooling}}(k)/\text{COP}\Delta k + P_{\text{fan}}(k)\Delta k, \forall k \in \mathcal{K}. \tag{13}$$

B. VB Models for Multi-zone HVAC

It is clear from (9a)-(9c) that the operation of multi-zone HVAC systems are governed by high-dimensional nonlinear state-space models, which are in contrast to the linear state-space models with single-zone cases. Particularly, the numbers of decision variables, operating constraints and the non-linear thermal dynamic equations grow with the number of thermal zones. As a result, the energy management tasks of multi-zone HVAC systems relying on the RC formulations often face substantial computational complexity. To this end, this

section extends the VB modeling framework to the multi-zone cases. We adopt the same *characterization state* to represent zone thermal conditions under thermal comfort constraints, i.e., $\text{soz}_{n,i}(k) = (T_{n,i}^{\text{set}} - T_{n,i}(k))/\delta_{n,i}, \forall i \in \mathcal{I}_n, k \in \mathcal{K}$. Similarly, we refer to maintaining zone temperature at their setpoints as `Baseline control`, leading to the following steady state equations by (11).

$$\boldsymbol{T}_n^{\text{set}}(k+1)=\boldsymbol{A}_n\boldsymbol{T}_n^{\text{set}}(k)-\boldsymbol{B}_n\boldsymbol{q}_n^{\text{base}}(k)+\boldsymbol{a}_n^{\text{out}}\boldsymbol{T}^{\text{out}}(k)+\boldsymbol{d}_n(k),$$
$$\boldsymbol{q}_n^{\text{base}}(k) = c_p \boldsymbol{m}_n(k)\left(\boldsymbol{T}_n^{\text{set}}(k) - \mathbf{1}_n T_n^{\text{sup}}\right), \forall k \in \mathcal{K}. \tag{14}$$

By subtracting (11) from (14) and dividing $\delta_{n,i}$ across the stacked equations, we have

$$\frac{T_{n,i}^{\text{set}}(k+1)-T_{n,i}(k)}{\delta_{n,i}}=a_{n,ii}\frac{T_{n,i}^{\text{set}}-T_{n,i}(k)}{\delta_{n,i}}+\sum_{j\in\mathcal{I}_n(i)}\frac{\delta_{n,j}}{\delta_{n,i}}\frac{T_{n,j}^{\text{set}}-T_{n,j}(k)}{\delta_{n,j}}$$
$$+\frac{b_{n,i}}{\delta_{n,i}}(q_{n,i}(k) - q_{n,i}^{\text{base}}(k)), \forall i \in \mathcal{I}_n, k \in \mathcal{K}. \tag{15}$$

By substituting (3) into (15), we have

$$\text{soz}_{n,i}(k + 1)=a_{n,ii}\text{soz}_{n,i}(k)+\sum_{j\in\mathcal{I}_n(i)}a_{n,ij}\frac{\delta_{n,j}}{\delta_{n,i}}\text{soz}_{n,j}(k)$$
$$+\frac{b_{n,i}}{\delta_{n,i}}(q_{n,i}(k) - q_{n,i}^{\text{base}}(k)), \forall i \in \mathcal{I}_n, k \in \mathcal{K}. \tag{16}$$

Finally, by stacking (16) across all zones, we have the following VB models for multi-zone HVAC systems:

Zone VB models for multi-zone HVAC system :

$$\begin{cases} \mathbf{soz}_n(k+1)=\tilde{\boldsymbol{A}}_n\mathbf{soz}_n(k)+\tilde{\boldsymbol{B}}_n(\boldsymbol{q}_n(k)-\boldsymbol{q}_n^{\text{base}}(k)) \\ -\mathbf{1}_n \leq \mathbf{soz}_n(k) \leq \mathbf{1}_n, \\ \boldsymbol{q}_n^{\min}(k) \leq \boldsymbol{q}_n(k) \leq \boldsymbol{q}_n^{\max}(k), \quad \forall k \in \mathcal{K}. \end{cases} \tag{17}$$

where we have

$$\tilde{\boldsymbol{A}}_n = \left[a_{n,ij}\delta_{n,j}/\delta_{n,i}\right]_{i,j\in\mathcal{I}_n} \in R^{I_n\times I_n},$$
$$\tilde{\boldsymbol{B}}_n = \text{diag}(b_{n,1}/\delta_{n,1}, \ldots, b_{n,N_n}/\delta_{n,I_n}) \in R^{I_n\times I_n}. \tag{18}$$

The accurate upper and low cooling power limits $\boldsymbol{q}_n^{\min}(k)$ and $\boldsymbol{q}_n^{\max}(k)$ are usually difficult to obtain as they are temporally coupled. Some simple and close estimations are

$$\hat{\boldsymbol{q}}_n^{\min}(k) = c_p \boldsymbol{m}_n^{\min}(k)\left(\boldsymbol{T}_n^{\text{set}}(k) - \mathbf{1}_n T_n^{\text{sup}}\right)$$
$$\hat{\boldsymbol{q}}_n^{\max}(k) = c_p \boldsymbol{m}_n^{\max}(k)\left(\boldsymbol{T}_n^{\text{set}}(k) - \mathbf{1}_n T_n^{\text{sup}}\right), k \in \mathcal{K}. \tag{19}$$

Remark 1. *In model* (17)*, the operating flexibility of multi-zone HVAC system has been represented by a series of virtual batteries, corresponding to individual zones. The zone thermal comfort constraints have been encoded by* $\text{soz}_{n,i} \in [-1,1], \forall i \in \mathcal{I}_n, k \in \mathcal{K}$*. This formulation enables flexible multi-zone buildings to function like virtual battery packs.*

C. Aggregated VB Model for Multi-zone HVAC

To reduce model and computational complexity, we further discuss how the zone VB models can be aggregated into a single VB at the building level. To achieve the objective, we first introduce the following important theorem to be used.

Theorem 1. *(Perron–Frobenius Theorem) Let $\boldsymbol{A} \in \boldsymbol{R}^{n \times n}$ be a non-negative matrix, i.e., $\boldsymbol{A}_{ij} \geq 0, \forall i, j$. Let $\rho(\boldsymbol{A})$ denote the spectral radius of $\boldsymbol{A}$, defined as*

$$\rho(\boldsymbol{A}) = \max \left\{|\lambda| : \lambda \text{ is an eigenvalue of } \boldsymbol{A}\right\},$$

then the following properties hold: (1) $\rho(\boldsymbol{A})$ is an eigenvalue of $\boldsymbol{A}$; (2) there exists a non-negative eigenvector $\boldsymbol{w}$ that $\boldsymbol{A}\boldsymbol{w} = \rho(\boldsymbol{A})\boldsymbol{w}$.

The parameters $\tilde{\boldsymbol{A}}_n$ and $\tilde{\boldsymbol{A}}_n^{\mathsf{T}}$ in (17) are real, non-negative and symmetric matrices, which can be readily verified. Hence, by **Theorem** 1, there exist a non-negative eigenvalue α_n and associated non-negative probability vector $\boldsymbol{w}_n$ of $\tilde{\boldsymbol{A}}_n^{\mathsf{T}}$ such that

$$\begin{aligned} \tilde{\boldsymbol{A}}_n^{\mathsf{T}} \boldsymbol{w}_n &= \alpha_n \boldsymbol{w}_n, \\ \boldsymbol{1}_n^{\mathsf{T}} \boldsymbol{w}_n &= 1. \end{aligned} \tag{20}$$

Specifically, the probability eigenvector $\boldsymbol{w}_n$ can be obtained by normalizing the eigenvector of $\tilde{\boldsymbol{A}}_n^{\mathsf{T}}$ associated with the non-negative eigenvalue α_n. To enable the aggregation of zone VB models, we further propose the following State-of-Charge (soc) as the *characterization state* of entire building thermal conditions under zone thermal comfort constraints:

$$\text{soc}_n(k) = \boldsymbol{w}_n^{\mathsf{T}} \mathbf{soz}_n(k), \quad \forall k \in \mathcal{K}. \tag{21}$$

Remark 2. *The soc can be interpreted as the aggregated thermal conditions of entire multi-zone building accounting for zone thermal comfort requirements. Notably, the physical heterogeneity of thermal zones has been encapsulated by the eigenvector $\boldsymbol{w}_n$, which enables the proposed modeling framework to be applicable to multi-zone buildings of heterogeneous zone typologies and envelopes.*

By multiplying both sides of (17) with $\boldsymbol{w}_n^{\mathsf{T}}$, we have

$$\begin{cases} \boldsymbol{w}_n^{\mathsf{T}} \mathbf{soz}_n(k+1) = \boldsymbol{w}_n^{\mathsf{T}} \tilde{\boldsymbol{A}}_n \mathbf{soz}_n(k) + \boldsymbol{w}_n^{\mathsf{T}} \tilde{\boldsymbol{B}}_n \left(\boldsymbol{q}_n(k) - \boldsymbol{q}_n^{\text{base}}(k)\right) \\ \quad - \boldsymbol{w}_n^{\mathsf{T}} \boldsymbol{1}_n \leq \mathbf{soz}_n(k) \leq \boldsymbol{w}_n^{\mathsf{T}} \boldsymbol{1}_n, \\ \boldsymbol{q}_n^{\min}(k) \leq \boldsymbol{q}_n(k) \leq \boldsymbol{q}_n^{\max}(k), \quad \forall k \in \mathcal{K}. \end{cases} \tag{22}$$

By plugging (20), (21) into (22), we obtain the following aggregated VB model for multi-zone HVAC systems:

$$\begin{cases} \text{soc}_n(k+1) = \alpha_n \text{soc}_n(k) + P_n^{\text{ch/dis}}(k) \\ \quad -1 \leq \text{soc}_n(k) \leq 1, \\ \boldsymbol{q}_n^{\min}(k) \leq \boldsymbol{q}_n(k) \leq \boldsymbol{q}_n^{\max}(k), \forall k \in \mathcal{K}. \end{cases} \tag{23}$$

where $P_n^{\text{ch/dis}}(k) \triangleq \boldsymbol{w}_n^{\mathsf{T}} \tilde{\boldsymbol{B}}_n \left(\boldsymbol{q}_n(k) - \boldsymbol{q}_n^{\text{base}}(k)\right), \forall k \in \mathcal{K}$ can be interpreted as the net charging power of the VB. One remaining problem is that the net charging power couples with the individual zone cooling power $\boldsymbol{q}_n(k) = [q_{n,i}(k)], \forall i \in \mathcal{I}_n$, which is not favored for building-level energy scheduling. We therefore propose to approximate the net charging power by

$$\begin{aligned} \beta_n^{\min}(k) \mathbf{I}_n^{\mathsf{T}} \boldsymbol{q}_n(k) &\leq \boldsymbol{w}_n^{\mathsf{T}} \tilde{\boldsymbol{B}}_n \boldsymbol{q}_n(k) \leq \beta_n^{\max}(k) \mathbf{I}_n^{\mathsf{T}} \boldsymbol{q}_n(k), \\ \boldsymbol{q}_n^{\min}(k) &\leq \boldsymbol{q}_n(k) \leq \boldsymbol{q}_n^{\max}(k), \forall k \in \mathcal{K}. \end{aligned} \tag{24}$$

where $\beta_n^{\min}(k)$ and $\beta_n^{\max}(k)$ are the lower and upper bound parameters to be identified. $\mathbf{I}_n^{\mathsf{T}} \boldsymbol{q}_n(k)$ represents the total cooling power of all zones. Many approaches can be used for the parameter estimations. Some conservative and tight bound parameters can be obtained as follows.

1) **Conservative bounds:** Since $\boldsymbol{w}_n$ is a nonnegative probability vector and $\tilde{\boldsymbol{B}}_n$ is a nonnegative diagonal matrix, the product $\boldsymbol{w}_n^T \tilde{\boldsymbol{B}}_n$ is a non-negative vector. We have the zone cooling power $\boldsymbol{q}_n(k)$ nonnegative and bounded, therefore a pair of bound parameters can be obtained by

$$\begin{aligned} \beta_n^{\min}(k) &= \min_i \left(\mathbf{w}_n^{\mathsf{T}} \tilde{\boldsymbol{B}}_n\right)_i, \\ \beta_n^{\max}(k) &= \max_i \left(\mathbf{w}_n^{\mathsf{T}} \tilde{\boldsymbol{B}}_n\right)_i, \quad \forall k \in \mathcal{K}. \end{aligned} \tag{25}$$

These bounds are conservative as they hold for all bounded control inputs regardless of the ranges of $\boldsymbol{q}_n(k)$.

2) **Tight bounds:** The tight and exact bound parameters correspond to the following optimization problems.

$$\begin{aligned} \beta_n^{\min}(k) &= \min_{\boldsymbol{q}_n(k) \in [\boldsymbol{q}_n^{\min}(k), \boldsymbol{q}_n^{\max}(k)]} \frac{\boldsymbol{w}_n^{\mathsf{T}} \tilde{\boldsymbol{B}}_n \boldsymbol{q}_n(k)}{\mathbf{I}_n^{\mathsf{T}} \boldsymbol{q}_n(k)} \\ \beta_n^{\max}(k) &= \max_{\boldsymbol{q}_n(k) \in [\boldsymbol{q}_n^{\min}(k), \boldsymbol{q}_n^{\max}(k)]} \frac{\boldsymbol{w}_n^{\mathsf{T}} \tilde{\boldsymbol{B}}_n \boldsymbol{q}_n(k)}{\mathbf{I}_n^{\mathsf{T}} \boldsymbol{q}_n(k)}, \forall k \in \mathcal{K}. \end{aligned} \tag{26}$$

The tight bounds exist and are available provided with the feasible ranges of $\boldsymbol{q}_n(k)$.

By plugging (24) into (22), we obtain the following aggregated VB model for multi-zone HVAC systems:

Aggregated VB model for multi-zone HVAC:

$$\begin{cases} \text{soc}_n(k+1) = \alpha_n \text{soc}_n(k) + P_n^{\text{ch/dis}}(k) \\ P_n^{\text{ch/dis}}(k) \geq \beta_n^{\min}(k) Q_n(k) - \boldsymbol{w}_n^{\mathsf{T}} \tilde{\boldsymbol{B}}_n \boldsymbol{q}_n^{\text{base}}(k) \\ P_n^{\text{ch/dis}}(k) \leq \beta_n^{\max}(k) Q_n(k) - \boldsymbol{w}_n^{\mathsf{T}} \tilde{\boldsymbol{B}}_n \boldsymbol{q}_n^{\text{base}}(k), \\ Q_n^{\min}(k) \leq Q_n(k) \leq Q_n^{\max}(k), \\ -1 \leq \text{soc}_n(k) \leq 1, \quad \forall k \in \mathcal{K}. \end{cases} \tag{27}$$

where $Q_n(k) \triangleq \mathbf{I}_n^{\mathsf{T}} \boldsymbol{q}_n(k)$ denotes the aggregated zone cooling power at time step k. According, we have $Q_n^{\min}(k) = \mathbf{I}_n^{\mathsf{T}} \boldsymbol{q}_n^{\min}(k)$ and $Q_n^{\max}(k) = \mathbf{I}_n^{\mathsf{T}} \boldsymbol{q}_n^{\max}(k)$ represent their lower and upper limits, and some estimations are $\hat{Q}_n^{\min}(k) = \mathbf{I}_n^{\mathsf{T}} \hat{\boldsymbol{q}}_n^{\min}(k)$ and $\hat{Q}_n^{\max}(k) = \mathbf{I}_n^{\mathsf{T}} \hat{\boldsymbol{q}}_n^{\max}(k)$.

Remark 3. *In model (27), the thermal dynamics, physical operating limits and thermal comfort constraints of multi-zone HVAC operation have been captured by a virtual battery storage representation, with $P_n^{\text{ch/dis}}(k), \text{soc}_n(k), Q_n(k)$ as decision variables and the others as static model parameters readily available from the RC formulations.*

When considering VB model (23) for building energy management and scheduling, an energy consumption model is necessary. This problem is nontrivial as the energy consumption of multi-zone HVAC system closely relates to zone-level control inputs and states (i.e., zone airflow rates, zone temperature), making it difficult to establish an analytic formulation at the aggregated level. To overcome the difficulty, this paper adopts a data-driven approach for energy consumption modeling. Specifically, it is clear from (12)-(13) that the system's energy consumption is determined by zone airflow rates $m_{n,i}(k)$, zone temperature $T_{n,i}(k)$, and the outdoor temperature $T^{\text{out}}(k)$. The zone-level control and state variables in fact have been

encapsulated by the aggregated states $\text{soc}_n(k)$ and aggregated control inputs $Q_n(k)$ with the VB model. Therefore, the energy consumption with VB model (23) can be captured by the following functional mappings

$$Q_n^{\text{tol}}(k) = \mathcal{F}\big(\text{soc}_n(k-L:k), Q_n(k-L:k),$$
$$T^{\text{out}}(k-L:k)\big), \quad \forall k \in \mathcal{K} \quad (28)$$

where $\mathcal{F}(\cdot)$ denotes a class of functional modules, such as neural networks or linear regression models. The hyperparameter L specifies the look-back window of historical information. We use $k-L:k$ to denote the time steps spanning from $k-L$ to k. This paper adopts the long short-term memory (LSTM) networks to capture the functional mappings considering their powerful representation capability.

Remark 4. *We have developed unified VB modeling framework for characterizing the operating flexibility of both single-zone and multi-zone building HVAC system, with the thermal comfort constraints encoded by $\text{soc} \in [-1, 1]$. In fact, the range of soc can be flexibly shifted to our requirements. Specifically, we are able to shift the ranges of soc to $[0, 1]$ with the VB models (7) and (27) by*

1) *Define the* characterization state *as*

$$\text{soz}_n(k) = \frac{T_n^{\max} - T_n(k)}{2\delta_n}, \quad \forall k \in \mathcal{K}. \quad (29)$$

where $T_n^{\max} \triangleq T_n^{\text{set}} + \delta_n, \forall k \in \mathcal{K}$ represent the upper zone comfortable temperature limits.

2) *Set the* Baseline control *as maintaining the zone temperature at the upper zone temperature limits $T_n^{\max}$.*

*The above are for single-zone HVAC systems and can be readily extended to multi-zone cases by introducing zone index i. Following the same modeling framework, we can obtain the same VB models (7) and (27) but with $\text{soc} \in [0, 1]$ and some slight modifications of model parameters. We refer readers to **Appendix** A and B for details.*

V. MODEL EVALUATION AND APPLICATIONS

In this part, we first evaluate the aggregated VB models for characterizing the aggregated thermal dynamics of multi-zone buildings. We then testing the VB models for DR participation of building HVAC systems in electricity market.

We consider a commercial multi-zone building with 5 thermal zones as illustrated in Fig. 2. The building thermal parameters and HVAC system configurations are summarized in TABLE II. The thermal disturbances and outdoor weather conditions are taken from the CityLearn datasets [31]. We set the decision and scheduling interval to be $\Delta k = 30$ mins with each day equally divided into $K = 48$ time slots.

A. SOC Model for characterizing building thermal dynamics

We first evaluate the VB models for characterizing building thermal dynamics under different control policies of the HVAC system. We first obtain the baseline cooling power trajectories $q_n^{\text{base}}(k), \forall k \in \mathcal{K}$ by solving the steady-state equations (14) to establish the VB model (27). We consider three representative control policies for the multi-zone HVAC system:

TABLE II: Building thermal parameters and HVAC system configurations

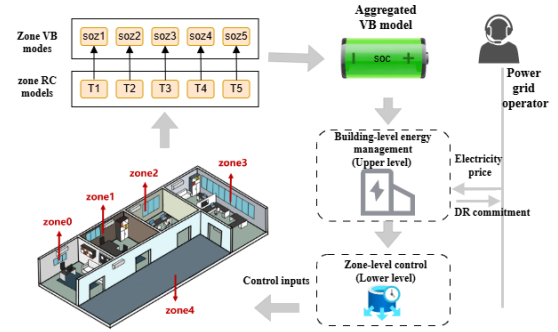| Param.	Value	Units
$C_{n,i}^{\text{th}}$ $(\forall i \in \mathcal{I}_n)$	1.5×10^4	J/(kg.K)
c_p	1.012	kJ/(kg.K)
d_r	0.8	–
$T_{n,i}^{\text{set}}$ $(\forall i \in \mathcal{I}_n)$	25	°C
$\delta_{n,i}$ $(\forall i \in \mathcal{I}_n)$	1	°C
$m_{n,i}^{\min}$ $(\forall i \in \mathcal{I}_n)$	0	kg/s
$m_{n,i}^{\max}$ $(\forall i \in \mathcal{I}_n)$	0.5	kg/s
$R_{n,ij}^{\text{th}}$ $(\forall i, j \in \mathcal{I}_n)$	14	kW/K
$R_{n,oi}^{\text{th}}$ $(\forall i \in \mathcal{I}_n)$	30	kW/K
κ_f	0.08	–
COP	1.0	–

Fig. 2: VB model for DR of multi-zone building HVAC system

- Random control: Randomly generating zone airflow rates within the operating ranges of VAV boxes for multi-zone HVAC system.
- PID control: Tuning a PID controller to modulate the zone airflow rates to keep the zone temperatures close to their respective comfort ranges.
- DRL control: Training a deep reinforcement learning (DRL) agent to control zone airflow rates with the objective minimizing the weighted sum of total electricity cost and comfortable zone temperature violations.

We simulate the three control policies on the RC model (11) to obtain the zone temperature $T_{n,i}(k)$ and cooling power trajectories $q_{n,i}(k)$. Each simulation spans 5 days ($K = 240$ time steps) to account for the uncertainties of thermal disturbances and weather conditions. Based on the simulated trajectories, we identify the actual soc trajectories soc^{true} for the building according to (3) and (21), which present the true aggregated thermal dynamics of the building under the control policy. We then compare the true soc^{true} with the soc obtained from the VB models for model evaluation.

We first establish the mappings from the control inputs of RC model to the VB model (27) to keep consistent operation. Specifically, for each simulated trajectory of the RC model, we have $Q_n(k) = \mathbf{1}^\top q_n(k)$ for the VB model. We consider three algorithms for estimating the model parameters $\beta_n^{\min}(k)$ and $\beta_n^{\max}(k)$:

- **Algorithm 1 (Conservative method):** Calculating $\beta_n^{\min}(k)$ and $\beta_n^{\max}(k), \forall k \in \mathcal{K}$ with the conservative

approach introduced in (25).

- **Algorithm 2 (Step-ahead estimation):** Estimating $\beta_n^{\min}(k)$ and $\beta_n^{\max}(k), \forall k \in \mathcal{K}$ using (26) by fixing $\boldsymbol{q}_n(k)$ to the zone cooling power $\boldsymbol{q}_n(k-1)$ obtained from previous time step.
- **Algorithm 3 (Optimal tight bounds)** Computing $\beta_n^{\min}(k)$ and $\beta_n^{\max}(k), \forall k \in \mathcal{K}$ according to (26) by setting $\boldsymbol{q}_n(k)$ to be the actual zone cooling power obtained with the RC model.

With the control inputs $Q_n(k), \forall k \in \mathcal{K}$ and the VB model parameters, we are able to simulate the soc trajectory of the multi-zone building with the VB model. However, one remaining issue is that, for the VB model (27), the soc is not uniquely determined by the control inputs $Q_n(k)$ due to the inequality relaxation (24). To handle this issue, we choose to evaluate the upper and lower bounds of soc for the given control inputs $Q_n(k)$:

$$\text{soc}^{\text{up}}(k+1) = \text{soc}^{\text{up}}(k) + P_n^{\text{ch/dis,up}}(k),$$
$$\text{soc}^{\text{dn}}(k+1) = \text{soc}^{\text{dn}}(k) + P_n^{\text{ch/dis,dn}}(k), \forall k \in \mathcal{K}.$$

where we have

$$P_n^{\text{ch/dis,up}}(k) = \beta_n^{\max}(k)Q_n(k) - \boldsymbol{w}_n^{\mathsf{T}} \tilde{\boldsymbol{B}}_n \boldsymbol{q}_n^{\text{base}}(k),$$
$$P_n^{\text{ch/dis,dn}}(k) = \beta_n^{\min}(k)Q_n(k) - \boldsymbol{w}_n^{\mathsf{T}} \tilde{\boldsymbol{B}}_n \boldsymbol{q}_n^{\text{base}}(k), \forall k \in \mathcal{K}.$$

Note that the differences between $\text{soc}^{\text{up}}(k)$ and $\text{soc}^{\text{dn}}(k)$ directly relate to the model parameters $\beta_n^{\min}(k)$ and $\beta_n^{\max}(k)$. We compare soc^{up} and soc^{dn} obtained from the VB models with soc^{true} to evaluate the the capability of VB models for capturing building thermal dynamics. We present the results for each control policy and the algorithm for model parameter estimations in Fig.3. It can be observed that the soc^{up} and soc^{dn} obtained from the VB models closely match the actual trajectories soc^{true} for almost all cases, demonstrating that the VB models can well capture the building thermal dynamics. Some gaps occur with the results of `Algorithm 1` (see Fig. 3 (a), (d), (g)), which are due to the quite conservative model parameters $\beta_n^{\min}(k)$ and $\beta_n^{\max}(k)$ provided by the method. These gaps can be effectively decreased by employing tighter model parameters $\beta_n^{\min}(k)$ and $\beta_n^{\max}(k)$ as can be seen from the results with `Algorithm 2` (see Fig. 3 (b), (e), (h)), in which the step-ahead estimation method is used and gives tighter model parameters. This conclusion has been further confirmed by the results of `Algorithm 3` (see Fig. 3 (e), (f), (i)), in which the optimal and tight model parameters are employed. As a result, the upper and lower soc trajectories soc^{up} and soc^{dn} exactly coincide with the actual soc^{true}. In such case, the proposed VB model is equivalent to the original RC model in characterizing building thermal dynamics.

The above results demonstrate that the VB models can well characterize the building thermal dynamics with sufficiently tight model parameters. Conservative model parameters may lead to certain accumulated gap in terms of soc trajectories, whereas it seems still applicable to many building-level energy management tasks as the accumulated gap is still quite minor for sufficiently long periods (see the previous 100 time steps of Fig. 3 (a), (d), (g)).

B. Energy Consumption Model for Multi-zone HVAC

We further evaluate the data-driven approach for energy consumption modeling with the VB model. We use a LSTM network (`layers: 1 seq length: 2, hidden dim: 64, batch size: 64`) combined with a fully connected layer to capture the functional mappings (28). We set the look-back window $L = 1$ as we observe that one-step historical information leads to the best model performance in the experiments. We first build datasets for model training, and then evaluate the model accuracy and generality. Specifically, we run the three control policies (i.e.,`Random control`, `PID control` and `DRL control`) using the RC model each spanning 100 days for data collection. For each simulated trajectory, the following state and control variables are evaluated and collected as samples:

$$\left(\text{soc}_n(k), Q_n(k), T^{\text{out}}(k), Q_n^{\text{tol}}(k)\right), \quad \forall k \in \mathcal{K}. \tag{30}$$

Based on the collected samples, we generate four datasets. Three datasets correspond directly to the trajectories produced by the three control policies and denoted as `Random control`, `PID control`, and `DRL control`, respectively. The fourth dataset, referred to as `Mixture control`, is obtained by uniformly concatenating segments from the three individual datasets. Note that the four datasets are of equal length, each of which contains 4.8K samples. We further divide each dataset by the ratio of $6 : 2 : 4$ for model training, validating and testing.

We then train four energy consumption models with the four datasets using the same LSTM architecture, and subsequently evaluate them on the same `Mixture Control` dataset. Particularly, we do not make any normalization on the datasets. Multiple widely-used metrics are employed to quantify the model performance and the results are reported in TABLE III. The best case in terms of each performance metric has been highlighted in bold text. First of all, we see that all the energy consumption models learned from the four datasets show favorable performance. The Pearson correlation coefficient (`Corr`) is quite close to 1. Meanwhile, the mean absolute percentage error (`MAPE`) are all less than 10%. By inspecting the performance metrics further, we observe that `Mixture control` dataset provides slightly better performance than the other three. This is reasonable as the `Mixture control` dataset is generated from three control policies and shows larger diversity in terms of system operation patterns.

We further evaluate the predictive performance of the trained models. We use the trained models to infer the energy consumption under different control policies, and compare them with the actual values. The results are presented in Fig. 4. Overall, all trained models demonstrate satisfactory predictive capability, and the model trained from the `Mixture control` dataset behaves the best, which is consistent with the performance metrics presented in TABLE III. Besides, it is important to note that all the trained models demonstrate satisfactory generality. Specifically, the models trained from the datasets generated from a specific control policy perform quite well in capturing the energy consumption of other control polices. This demonstrates the effectiveness of the data-driven
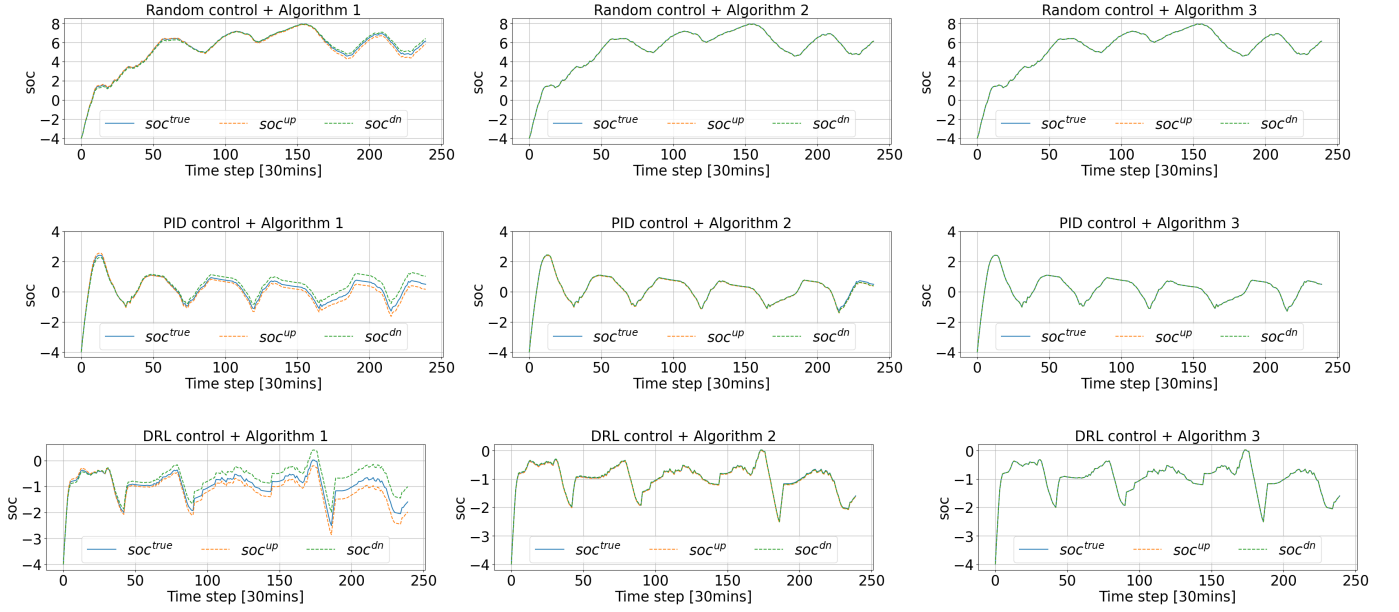
Fig. 3: The actual soc from the RC model and the upper and low soc from the VB model under different control policies (`Random control`, `PID control`, `DRL control`) and methods (`Algorithm 1`, `Algorithm 2`, `Algorithm 3`) for estimating model parameters $\beta_n^{\min}(k)$ and $\beta_n^{\max}(k)$.

approach in modeling the energy consumption of multi-zone HVAC systems with the VB model.

TABLE III: Performance of trained energy consumption models for multi-zone HVAC system

Datasets (Training)	Mixture control (Testing)					
	MAPE [%]	RMSE [kW]	MAE [kW]	RSE [%]	RAE [%]	Corr [0, 1]
Random control	7.89	**0.6606**	0.5101	**10.37**	9.49	**0.9954**
PID control	5.36	1.0162	0.5704	15.95	10.61	0.9918
DRL control	7.75	1.5334	0.8644	24.06	16.08	0.9794
Mixture control	**4.51**	0.7358	**0.4294**	11.55	**7.99**	0.9944

C. VB model for Building Demand Response (DR)

In this part, we apply the VB model for DR participation of the multi-zone building in electricity market. Specifically, we consider Time-of-Use (ToU) electricity price and study how the control flexibility of the multi-zone HVAC system can be exploited to reduce the building's electricity cost. This problem can be modeled as a hierarchical control problem: the `upper level` determines the DR commitment of the multi-zone building HVAC system and the `lower level` divides the DR commitment to zone-level control inputs when called by the power grid operator. The `upper level` DR commitment can be made by using the proposed VB model with the following problem formulation:

$$\hat{\mathbf{X}} = \arg\min_{\mathbf{X}} \sum_{k \in \mathcal{K}} c(k) \cdot Q_n^{\text{tol}}(k) \quad \text{s.t. } (27) - (28). \tag{31}$$

where $\mathbf{X} \triangleq [\text{soc}_n(k), P_n^{\text{ch/dis}}(k), Q_n(k), Q_n^{\text{tol}}(k)], \forall k \in \mathcal{K}$ are decision variables. $c(k), \forall k \in \mathcal{K}$ denote the ToU electricity

price. The model parameters $\beta_n^{\min}(k)$ and $\beta_n^{\max}(k)$ are computed using the conservative method of `Algorithm 1`. The resulted DR commitment is denoted by $[\hat{Q}_n^{\text{tol}}(k)], \forall k \in \mathcal{K}$, which represents the committed energy consumption trajectory of the HVAC system over the DR window $\mathcal{K}$.

When the committed DR is called by power grid operator, the `lower level` requires to decompose the DR strategy to zone-level control inputs. This can be formulated as tracking the committed energy consumption trajectory $\hat{Q}_n^{\text{tol}}(k)$ as close as possible while respecting the operating limits and thermal comfort constraints:

$$\hat{\mathbf{Y}}^* = \arg\min_{\mathbf{Y}} \sum_{k \in \mathcal{K}} \left(Q_n^{\text{tol}}(k) - \hat{Q}_n^{\text{tol}}(k) \right)^2 \tag{32}$$
$$\text{s.t. } (9a) - (9c), (12) - (13).$$

where $\mathbf{Y} \triangleq [m_{n,i}(k), T_{n,i}(k), q_{n,i}(k), Q_n^{\text{tol}}(k)], \forall i \in \mathcal{I}_n, k \in \mathcal{K}$ denote the decision variables. The `lower level` uses RC model to obtain zone-level control inputs. We denote the resulted actual energy consumption trajectory of HVAC system as $\hat{\mathbf{Q}}_n^{\text{tol},*}(k), \forall k \in \mathcal{K}$. The actual electricity cost for DR participation is evaluated as $\text{Cost}_{\text{VB}} = \sum_{k \in \mathcal{K}} c(k) \cdot \hat{Q}_n^{\text{tol},*}(k)$.

We evaluate the effectiveness of the VB model for DR participation by comparing the electricity cost Cost_{VB} with the theoretical optima Cost_{Opt}, which can obtained by solving the optimization problem (32) with the objective replaced by that of (31). We consider electricity markets with different DR commitment windows, including 1 day, 3 days and 5 days (i.e., $K = 48, 144, 240$). For each case, $S = 30$ independent experiments are performed to account for the uncertainties. We calculate the average electricity cost of $S = 30$ experiments and use it as performance metrics. In addition to electricity cost, we also evaluate the model complexity by the number of
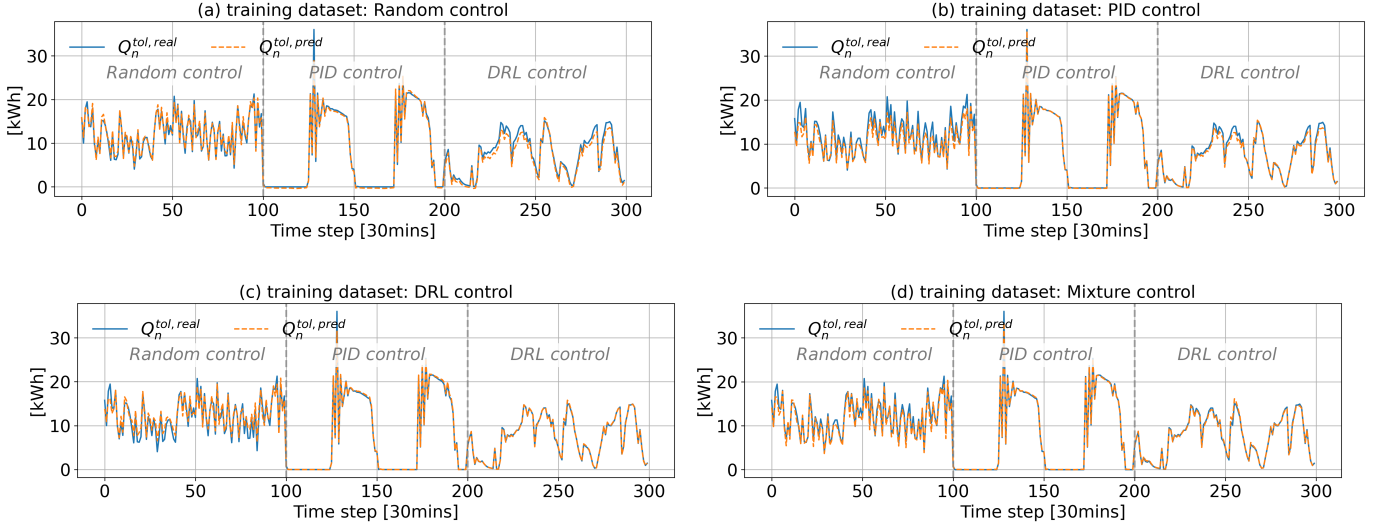
Fig. 4: Predictive performance of energy consumption models trained from different datasets: (a) `Random control`, (b) `PID control`, (c) `DRL control` testing on the `Mixture control` dataset.

decision variables involved. Particularly, we only focus on DR commitments and thus only evaluate the model complexity of `upper level` for the VB model. The results of all case studies are summarized in TABLE IV. We note that there only exist minor performance gaps (about 5%) in terms of the average electricity cost with the VB model compared with the theoretical optima. Moreover, we see that the performance of VB model for DR commitment is quite stable under different DR windows. The results demonstrate that the conservative model parameters $\beta_n^{\min}(k)$ and $\beta_n^{\min}(k)$ are sufficient for effective DR participation of buildings. Besides, it is important to note that the VB model can enable considerable model complexity reduction compared with RC model. Specifically, the number of decision variables with the VB model only linearly increase with the optimization horizon regardless the number of thermal zones involved, whereas the number of decision variables increases both with the number of zones and the optimization horizon with the RC model. This is because the zone operating flexibility has been aggregated by the VB model. Moreover, the VB model admits a linear state-space model, which is in contrast to the nonlinear state-space model with the RC model. Therefore, the VB model favors building-level energy management and scheduling considering the model and computational complexity.

TABLE IV: Performance of DR for multi-zone HVAC systems under different DR commitment windows

| Optimization Horizon [Steps] | RC model | | VB model | | |
	Cost_{Opt} (Avg.) [\$]	# Decision variable	Cost_{VB} (Avg.) [\$]	# Decision variable	Performance Gap [%]
48 (1 day)	57.71	480	61.08	144	5.7%
144 (3 days)	194.14	1440	201.14	432	3.7%
240 (5 days)	328.39	2400	339.44	720	3.4%

To further demonstrate the favorable performance of VB

models for DR participation, we compare the electricity cost distribution of the $S = 30$ experiments obtained from the VB model with the theoretical optima. The results are presented in Fig. 5. We see that for the different DR commitment windows, the electricity cost distributions with the VB model are quite close to the theoretical optima. This demonstrates that the proposed VB model can provide near-optimal and stable performance for DR participation under uncertainties and varying DR commitment windows.

Fig. 5: Electricity cost distributions of VB model and theoretical optima in electricity markets with different DR commitment windows: (a) $K = 48$ (1 day), (b) $K = 144$ (3 days), (c) $K = 240$ (5 days).

Another novel benefit of the VB model is that it enables flexible buildings to function like virtual batteries. To examine this behavior, we investigate the soc of multi-zone HVAC system under varying DR prices. We randomly select five days from the $S = 30$ experiments of different DR commitment windows and present the building soc trajectories in Fig. 6. We can observe an obvious inverse patterns in terms of building soc and DR price fluctuations. Specifically, we generally see an increasing soc at low price and a decreasing soc at high price. Moreover, we see that the soc has been maintained within the range of $[-1, 1]$. This actually indicates that the building has leveraged the operational flexibility of multi-zone HVAC system in response of dynamic electricity price.
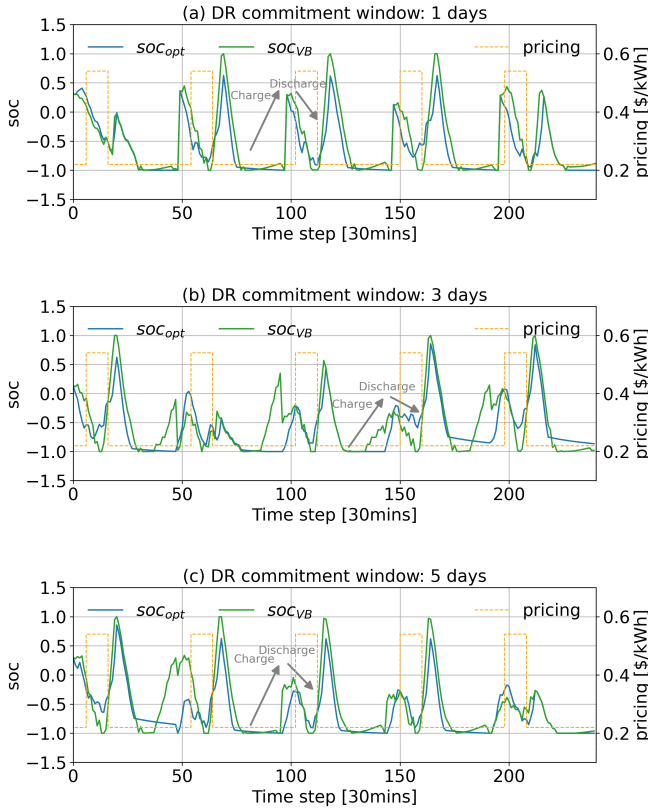

Fig. 6: The dynamic soc of multi-zone HVAC system in response to DR price in electricity markets with different DR commitment windows: (a) $K = 48$ (1 day), (b) $K = 144$ (3 days), (c) $K = 240$ (5 days).

VI. Conclusion

This paper developed a unified virtual battery (VB) modeling framework for characterizing the operating flexibility of both single-zone and multi-zone HVAC systems. The proposed VB models were established from the widely-used RC formulations with theoretic guarantee. The proposed VB models show high interpretability and enable flexible buildings to function like virtual batteries. We demonstrated the effectiveness of VB models for characterizing building thermal dynamics and their near-optimal performance for building demand response (DR) applications. The VB models are applicable to diverse building-level energy management or scheduling tasks and provide a solid model foundation for unlocking the substantial operating flexibility of buildings for supporting modern power grid operation. Several promising future directions have been identified. First, it is interesting to integrate the VB model into the deep reinforcement learning framework and explore whether a low-order model can accelerate the learning rate and lead to better building energy management strategies. Second, the VB model can be further extended for aggregating the operating flexibility of building clusters for providing grid service at the microgrid or city level.

Appendix A

For single-zone HVAC, the characterization state is

$$\text{soz}_n(k) = \frac{T_n^{\max} - T_n(k)}{2\delta_n}, \quad \forall k \in \mathcal{K}. \tag{33}$$

When the HVAC unit is operated under `Baseline control`, i.e., maintaining the zone temperature at the upper temperature limit, we have the following steady-state equations according to (1a):

$$T_n^{\max}(k+1) = a_n T_n^{\max}(k) - b_n q_n^{\text{HVAC,base}}(k) + d_n(k), \forall k \in \mathcal{K}. \tag{34}$$

By subtracting (1a) from (34), and dividing $2\delta_n$, we have

$$\begin{aligned} \frac{T_n^{\max}(k+1) - T_n(k+1)}{2\delta_n} &= a_n \frac{T_n^{\max}(k) - T_n(k+1)}{2\delta_n} \\ &+ b_n \frac{q_n^{\text{HVAC,base}}(k) - q_n^{\text{HVAC}}(k)}{2\delta_n}, \forall k \in \mathcal{K}. \end{aligned} \tag{35}$$

By substituting (34) into (35), and combine with the HVAC operating limits and thermal comfort constraints, we obtain the following VB model for single-zone HVAC system:

VB model for-single-zone HVAC:

$$\begin{cases} \text{soz}_n(k+1) = a_n \text{soz}_n(k) + P_n^{\text{ch/dis}}(k), \\ q_n^{\text{HVAC,min}}(k) \leq q_n^{\text{HVAC}}(k) \leq q_n^{\text{HVAC,max}}(k), \\ 0 \leq \text{soz}_n(k) \leq 1, \forall k \in \mathcal{K}. \end{cases} \tag{36}$$

where $P_n^{\text{ch/dis}}(k) = b_n/(2\delta_n)\left(q_n^{\text{HVAC}}(k) - q_n^{\text{HVAC,base}}(k)\right)$ denotes the net charging energy of the VB model at time step k. The energy consumption of the HVAC at time step k is $q_n^{\text{HVAC}}(k)\Delta k$, which can be equivalently expressed as $Q_n^{\text{tol}}(k) = \left(2P_n^{\text{ch/dis}}(k)\delta_n/b_n + q_n^{\text{HVAC,base}}(k)\right)\Delta k$ with the VB model.

Appendix B

For multi-zone HVAC, the characterization states are

$$\text{soz}_{n,i}(k) = \frac{T_{n,i}^{\max} - T_{n,i}(k)}{2\delta_{n,i}}, \quad \forall i \in \mathcal{I}_n, k \in \mathcal{K}. \tag{37}$$

When the system is operating under `Baseline control`: maintaining the zone to the upper comfortable temperature limits $T_{n,i}^{\max} \triangleq T_{n,i}^{\text{set}} + \delta_{n,i}$, we have the following steady-state equations according to (11):

$$\boldsymbol{T}_n^{\max}(k+1) = \boldsymbol{A}_n \boldsymbol{T}_n^{\max}(k) + \boldsymbol{B}_n \boldsymbol{q}_n^{\text{base}}(k) + \boldsymbol{a}_n^{\text{out}} \boldsymbol{T}^{\text{out}}(k) + \boldsymbol{d}_n(k),$$
$$\boldsymbol{q}_n^{\text{base}}(k) = c_p \boldsymbol{m}_n(k)\left(\boldsymbol{T}_n^{\max}(k) - \boldsymbol{1}_{N_n} T_n^{\text{sup}}\right), \forall k \in \mathcal{K}. \tag{38}$$

By subtracting (11) from (38), and dividing $2\delta_{n,i}$ for each of the stacked equations, we have

$$\frac{T_{n,i}^{\max}(k+1) - T_{n,i}(k)}{2\delta_{n,i}} = a_{n,ii}\frac{T_{n,i}^{\max} - T_{n,i}(k)}{2\delta_{n,i}}$$
$$+ \sum_{j \in \mathcal{I}_n(i)} \frac{\delta_{n,j}}{\delta_{n,i}}\frac{T_{n,j}^{\max} - T_{n,j}(k)}{2\delta_{n,j}} + \frac{b_{n,i}}{2\delta_{n,i}}(q_{n,i}(k) - q_{n,i}^{\text{base}}(k)), \quad (39)$$
$$\forall i \in \mathcal{I}_n, k \in \mathcal{K}.$$

By substituting (29) into (39), we further have

$$\text{soz}_{n,i}(k+1) = a_{n,ii}\text{soz}_{n,i}(k) + \sum_{j \in \mathcal{I}_n(i)} a_{n,ij}\frac{\delta_{n,j}}{\delta_{n,i}}\text{soz}_{n,j}(k)$$
$$+ \frac{b_{n,i}}{2\delta_{n,i}}(q_{n,i}(k) - q_{n,i}^{\text{base}}(k)), \quad \forall i \in \mathcal{I}_n, k \in \mathcal{K}. \quad (40)$$

By stacking (40) across all zones, we obtain the VB models for multi-zone HVAC systems:

Zone VB models for multi-zone HVAC system:

$$\begin{cases} \mathbf{soz}_n(k+1) = \tilde{\boldsymbol{A}}_n\mathbf{soz}_n(k) + \tilde{\boldsymbol{B}}_n\big(\boldsymbol{q}_n(k) - \boldsymbol{q}_n^{\text{base}}(k)\big) \\ \mathbf{0}_n \le \mathbf{soz}_n(k) \le \mathbf{1}_n, \\ \boldsymbol{q}_n^{\min}(k) \le \boldsymbol{q}_n(k) \le \boldsymbol{q}_n^{\max}(k), \quad \forall k \in \mathcal{K}. \end{cases} \quad (41)$$

where we have

$$\tilde{\boldsymbol{A}}_n = \begin{bmatrix} a_{n,11} & a_{n,12}\frac{\delta_{n,2}}{\delta_{n,1}} & \cdots & a_{n,1N_n}\frac{\delta_{n,N_n}}{\delta_{n,1}} \\ a_{n,21}\frac{\delta_{n,1}}{\delta_{n,2}} & a_{n,22} & \cdots & a_{n,2N_n}\frac{\delta_{n,N_n}}{\delta_{n,2}} \\ \vdots & \vdots & \ddots & \vdots \\ a_{n,N_n1}\frac{\delta_{n,1}}{\delta_{n,N_n}} & a_{n,N_n2}\frac{\delta_{n,2}}{\delta_{n,N_n}} & \cdots & a_{n,N_nN_n} \end{bmatrix} \in R^{I_n \times I_n},$$

$$\tilde{\boldsymbol{B}}_n = \text{diag}\left(\frac{b_{n,1}}{2\delta_{n,1}}, \ldots, \frac{b_{n,N_n}}{2\delta_{n,N_n}}\right) \in R^{I_n \times I_n},$$
$$\mathbf{0}_n = [0, 0, \cdots, 0] \in R^{I_n}, \mathbf{1}_n = [1, 1, \cdots, 1] \in R^{I_n}. \quad (42)$$

Subsequently, by following the proposed multi-zone VB aggregation framework in Section IV-D, we can obtain the aggregated VB model for building multi-zone HVAC systems:

Aggregated VB model for multi-zone HVAC:

$$\begin{cases} \text{soc}_n(k+1) = \alpha_n\text{soc}_n(k) + P_n^{\text{ch/dis}}(k), \\ P_n^{\text{ch/dis}}(k) \ge \beta_n^{\min}(k)Q_n(k) - \boldsymbol{w}_n^{\mathsf{T}}\tilde{\boldsymbol{B}}_n\boldsymbol{q}_n^{\text{base}}(k), \\ P_n^{\text{ch/dis}}(k) \le \beta_n^{\max}(k)Q_n(k) - \boldsymbol{w}_n^{\mathsf{T}}\tilde{\boldsymbol{B}}_n\boldsymbol{q}_n^{\text{base}}(k), \\ Q_n^{\min}(k) \le Q_n(k) \le Q_n^{\max}(k), \\ 0 \le \text{soc}_n(k) \le 1, \quad \forall k \in \mathcal{K}. \end{cases} \quad (43)$$

The energy consumption model can be established using the same data-driven approach introduced in (28) with the VB model.

REFERENCES

[1] International Energy Agency, "Energy efficiency 2025," 2025. Licence: CC BY 4.0.

[2] S. Wijesuriya, R. A. Kishore, M. Mitchell, and C. Booten, "Enhancing energyplus capabilities to model dynamic building envelopes using python plugin," *Energy and Buildings*, p. 115776, 2025.

[3] A. Roth *et al.*, "Grid-interactive efficient buildings: Whole-building controls, sensors, modeling, and analytics," Tech. Rep. NREL/TP–5500-75478; DOE/GO–102019-5230, U.S. Department of Energy, Building Technologies Office; National Renewable Energy Laboratory, 2019.

[4] X. Kou, Y. Du, F. Li, H. Pulgar-Painemal, H. Zandi, J. Dong, and M. M. Olama, "Model-based and data-driven hvac control strategies for residential demand response," *IEEE Open Access Journal of Power and Energy*, vol. 8, pp. 186–197, 2021.

[5] C. Anuntasethakul and D. Banjerdpongchai, "Design of supervisory model predictive control for building hvac system with consideration of peak-load shaving and thermal comfort," *IEEE access*, vol. 9, pp. 41066–41081, 2021.

[6] F. A. Qureshi and C. N. Jones, "Hierarchical control of building hvac system for ancillary services provision," *Energy and Buildings*, vol. 169, pp. 216–227, 2018.

[7] J. Drgoňa, J. Arroyo, I. C. Figueroa, D. Blum, K. Arendt, D. Kim, E. P. Ollé, J. Oravec, M. Wetter, D. L. Vrabie, *et al.*, "All you need to know about model predictive control for buildings," *Annual reviews in control*, vol. 50, pp. 190–232, 2020.

[8] U.S. Department of Energy and Lawrence Berkeley National Laboratory, "Energyplus energy simulation software." https://energyplus.net/, 2025. Version X.Y.Z (replace with the version you used).

[9] S. A. Klein, W. A. Beckman, J. A. Duffie, *et al.*, "Trnsys: A transient system simulation program." http://sel.me.wisc.edu/trnsys, 2017. Solar Energy Laboratory, University of Wisconsin–Madison.

[10] F. Smarra, A. Jain, T. De Rubeis, D. Ambrosini, A. D'Innocenzo, and R. Mangharam, "Data-driven model predictive control using random forests for building energy optimization and climate control," *Applied energy*, vol. 226, pp. 1252–1272, 2018.

[11] S. Lu, W. Gu, S. Ding, S. Yao, H. Lu, and X. Yuan, "Data-driven aggregate thermal dynamic model for buildings: A regression approach," *IEEE Transactions on Smart Grid*, vol. 13, no. 1, pp. 227–242, 2021.

[12] K. Deng, P. Barooah, P. G. Mehta, and S. P. Meyn, "Building thermal model reduction via aggregation of states," in *Proceedings of the 2010 American Control Conference*, pp. 5118–5123, IEEE, 2010.

[13] M. Maasoumy, A. Pinto, and A. Sangiovanni-Vincentelli, "Model-based hierarchical optimal control design for hvac systems," in *Dynamic systems and control conference*, vol. 54754, pp. 271–278, 2011.

[14] Y. Yang, S. Srinivasan, G. Hu, and C. J. Spanos, "Distributed control of multizone hvac systems considering indoor air quality," *IEEE Transactions on Control Systems Technology*, vol. 29, no. 6, pp. 2586–2597, 2021.

[15] Y. Yang, G. Hu, and C. J. Spanos, "Hvac energy cost optimization for a multizone building via a decentralized approach," *IEEE Transactions on Automation Science and Engineering*, vol. 17, no. 4, pp. 1950–1960, 2020.

[16] X. Cui, S. Liu, G. Ruan, and Y. Wang, "Data-driven

aggregation of thermal dynamics within building virtual power plants," *Applied Energy*, vol. 353, p. 122126, 2024.

[17] X. Cui, Y. Wang, and B. Xu, "Dimension-reduced optimization of multi-zone thermostatically controlled loads," *IEEE Transactions on Smart Grid*, 2025.

[18] H. Hao, D. Wu, J. Lian, and T. Yang, "Optimal coordination of building loads and energy storage for power grid and end user services," *IEEE Transactions on Smart Grid*, vol. 9, no. 5, pp. 4335–4345, 2017.

[19] L. Zhao, W. Zhang, H. Hao, and K. Kalsi, "A geometric approach to aggregate flexibility modeling of thermostatically controlled loads," *IEEE Transactions on Power Systems*, vol. 32, no. 6, pp. 4721–4731, 2017.

[20] K. Mukhi and A. Abate, "Aggregate flexibility of thermostatically controlled loads using generalized polymatroids," *arXiv preprint arXiv:2504.00484*, 2025.

[21] Z. Hou, S. Lu, Y. Xu, H. Qiu, W. Gu, Z. Y. Dong, and S. Ding, "Privacy-preserved aggregate thermal dynamic model of buildings," *IEEE Transactions on Smart Grid*, vol. 15, no. 6, pp. 5653–5664, 2024.

[22] M. Song, C. Gao, H. Yan, and J. Yang, "Thermal battery modeling of inverter air conditioning for demand response," *IEEE Transactions on Smart Grid*, vol. 9, no. 6, pp. 5522–5534, 2017.

[23] M. Song, W. Sun, Y. Wang, M. Shahidehpour, Z. Li, and C. Gao, "Hierarchical scheduling of aggregated tcl flexibility for transactive energy in power systems," *IEEE Transactions on Smart Grid*, vol. 11, no. 3, pp. 2452–2463, 2019.

[24] X. Zhu, P. Wang, N. Li, and W. Yan, "Multi-period optimal scheduling of building loads based on accurate virtual battery model," *Energy and Buildings*, vol. 327, p. 115046, 2025.

[25] A. Abbas, R. Ariwoola, B. Chowdhury, S. Kamalasadan, and Y. Lin, "Evaluation of equivalent battery model representations for thermostatically controlled loads in commercial buildings," in *2022 IEEE Industry Applications Society Annual Meeting (IAS)*, pp. 1–6, IEEE, 2022.

[26] Z. Guo, A. R. Coffman, J. Munk, P. Im, and P. Barooah, "Identification of aggregate building thermal dynamic model and unmeasured internal heat load from data," in *2019 IEEE 58th Conference on Decision and Control (CDC)*, pp. 2958–2963, IEEE, 2019.

[27] Z. Guo, A. R. Coffman, J. Munk, P. Im, T. Kuruganti, and P. Barooah, "Aggregation and data driven identification of building thermal dynamic model and unmeasured disturbance," *Energy and Buildings*, vol. 231, p. 110500, 2021.

[28] D. Qiu, J. Xue, T. Zhang, J. Wang, and M. Sun, "Federated reinforcement learning for smart building joint peer-to-peer energy and carbon allowance trading," *Applied Energy*, vol. 333, p. 120526, 2023.

[29] Y. Lin, P. Barooah, S. Meyn, and T. Middelkoop, "Experimental evaluation of frequency regulation from commercial building hvac systems," *IEEE Transactions on Smart Grid*, vol. 6, no. 2, pp. 776–783, 2015.

[30] Z. Wang, G. Hu, and C. J. Spanos, "Distributed model predictive control of bilinear hvac systems using a convexification method," in *2017 11th Asian control conference (ASCC)*, pp. 1608–1613, IEEE, 2017.

[31] K. Nweye, K. Kaspar, G. Buscemi, T. Fonseca, G. Pinto, D. Ghose, S. Duddukuru, P. Pratapa, H. Li, J. Mohammadi, *et al.*, "Citylearn v2: energy-flexible, resilient, occupant-centric, and carbon-aware management of grid-interactive communities," *Journal of Building Performance Simulation*, vol. 18, no. 1, pp. 17–38, 2025.